Bacterial Cellulose as a Carbon Nano-fiber Precursor: Enhancement of Thermal Stability and Electrical Conductivity

Fateme Rezaei,[a] Rabi Behrooz,[a,*] Shahram Arbab,[b] and Ehsanollah Nosratian Sabet [c]

Bacterial cellulose was selected as a potential precursor for the production of carbon nanofiber because of its high purity and crystallinity. Diammonium phosphate ($(NH_4)_2HPO_4$) as a flame retardant was used to impregnate the cellulosic nanofiber sheet precursor in order to increase its thermal stability during the thermal processing. Also, the effect of heating rate on the stabilization and carbonization processes of cellulosic nanofiber samples was investigated. The precursor and resulted carbon nanofiber sheets were characterized by scanning electron microscopy (SEM), Fourier transform infrared spectroscopy (FTIR), x-ray diffraction (XRD), thermogravimetric analysis (TGA), differential scanning calorimetry (DSC), and electrical characteristics. The results showed that the simultaneous usage of flame retardant (diammonium phosphate) and low heating rate in the stabilization process (2 °C min^{-1}) increases thermal stability of cellulosic nanofiber sheets and the carbon yield. The presence of a flame retardant acts like a low heating rate effect but does not significantly affect the high heating rate of the stabilization process. As carbonization temperature increased, electrical conductivity and crystallite size were increased for impregnated samples. The carbonization process at 1200 °C, with a heating rate of 2 °C min^{-1}, makes bacterial cellulose precursor an appropriate candidate for producing carbon nanofiber sheets with proper electrical characteristics.

Keywords: Bacterial cellulose; Carbon nano fiber; Electrical conductivity; Thermal stability

*Contact information: a: Department of Wood and Paper Science and Technology, Faculty of Natural Resources, Tarbiat Modares University, Iran; b: ATMT Research Institute, AmirKabir University of Technology, Tehran 15875-4413, Iran; c: Department of Textile Engineering, Amirkabir University of Technology, Tehran 15875-4413, Iran; *Corresponding author: Rabi.behrooz@modares.ac.ir*

INTRODUCTION

Cellulosic precursors, as a type of renewable biopolymer for production of carbon fiber, are used because of low cost and due to their mechanical flexibility and high electrical conductivity of resulting carbon fiber (Wu and Pan 2002; Peng *et al.* 2003; Dumanli and Windle 2012). Plants are not desirable as the main sources of cellulose for direct production of carbon fibers due to discontinuous string structure, high impurity, and low degree of orientation (Donnet and Bansal 1984). Therefore, regenerated cellulose fibers manufactured by multiple chemical complex processes can be used for production of carbon fibers (Chanzy *et al.* 1990; Wu and Pan 2002; Zhang *et al.* 2006; Koslow 2007).

In recent years, a new nanoscale source of cellulose, namely bacterial cellulose (BC), has been introduced. The fibril shape of bacterial cellulose produced by some bacteria offers several important properties, including chemical purity, nanostructure based on glucose monomer, high degree of polymerization, high mechanical strength, and high crystallinity (El-Saied *et al.* 2004; Chen *et al.* 2010; Saibuatong and Phisalaphong

2010; Dahman *et al.* 2010; Castro *et al.* 2011; Keshk 2014). Therefore, bacterial cellulose has a superior potential for producing carbon nanofiber without any excess treatment (Zhu *et al.* 2010; Shah 2013).

These features make BC an attractive material for a wide range of applications, including biomedicines, food technology, the packaging industry, the pulp and paper industry, as well as in the engineering of electrical appliances. Therefore, BC is considered as one of the most important and innovative materials for rapidly advancing industries (Abba *et al.* 2019; Salihu *et al.* 2019).

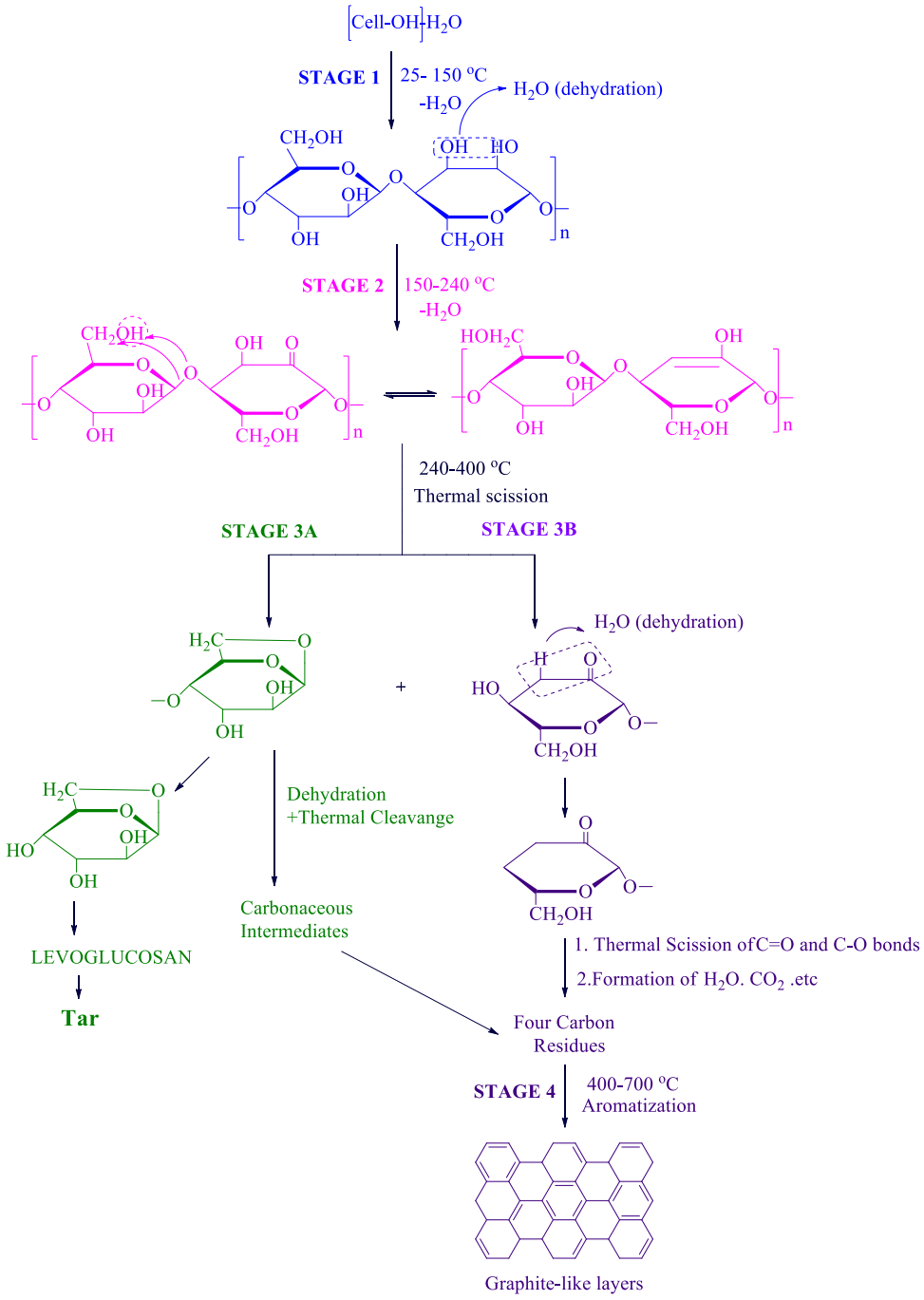

Fig. 1. The mechanism of cellulose pyrolysis (Tang and Bacon 1964)

Cellulosic precursors undergo stabilization and carbonization processes as they are being converted to carbon fibers. Stabilization is a crucial step in the production of cellulose-based carbon fibers (Arbab and Zeinolebadi 2013; Mirbaha *et al.* 2013; Arbab *et al.* 2014, 2017; Rafiei *et al.* 2014; Nosratian Sabet *et al.* 2016), during which several reactions take place at the same time. The precursor is stabilized as a result of chemical and physical changes for the subsequent carbonization process that is done at higher temperatures. As the temperature is raised, the cellulosic structure breaks down into highly volatile gases and carbon char (Frank *et al.* 2014).

At the beginning of thermal treatment, physical desorption of water and dehydration of the cellulosic unit occur up to about 240 °C (Tang and Bacon 1964). At the elevated temperatures, cellulose depolymerization occurs with thermal scission in glycosylated units, which leads to formation of large amounts of volatile products at about 400 °C. Therefore, keeping the temperature below 250 °C in the initial stages of thermal treatment and controlling the heating rate are necessary to improve carbon yield and prevent the formation of undesirable levoglucosan (Kilzer and Broido 1965; Madorsky 1967) (Fig. 1, stage 3a). The scheme of cellulose pyrolysis is shown in Fig. 1.

The thermal stability of various cellulose sources depends on the process conditions in the production of cellulose fibers. There are two solutions to this: 1.) The first solution is treatment of the cellulose precursor with flame retardants, which enhances thermal stability of cellulosic precursors during the pyrolysis process and reduces the rate of chemical decomposition reactions. 2.) The second solution is using low heating rates in the stabilization process, which can have a significant effect on the thermal stability of samples (Dumanli and Windle 2012; Frank *et al.* 2014).

Consequently, any procedure that lessens the depolymerization process compared with the dehydration process would promote stability of cellulose and it can be advantageous for production of carbon fibers.

Several researchers have reported that pyrolysis of cellulose in the presence of flame retardant can be accomplished at lower temperatures and produces high carbon char content (Schuyten *et al.* 1955; Shindo *et al.* 1969; Li *et al.* 2007; Weil and Levchik 2008; Frank *et al.* 2014).

The most common flame retardants include phosphoric acid, $(NH_4)_2SO_4$ and organosilicon, which may be impregnated solutions in water. Other possible flame retardants are aqueous solutions of nitrogen salts of strong acids (NH_4Cl), urea, Cs, Na, and K salts (Na_2CO_3), Fe^{2+} and Fe^{3+}, alkyl, aryl and halogenated alkyl or aryl phosphates, phosphates, phosphazenes, phosphonates, and polyphosphonates (Lewin 2006), but using some of them may be restricted due to toxicological and ecological problems.

Lyocell (as Tencel®) and viscose rayon fibers were used as precursors of carbon fiber by several researchers (Statheropoulos *et al.* 2000; Pappa *et al.* 2003; Goldhalm and Lenzinger 2012; Karacan and Soy 2013; Sporl *et al.* 2017). These precursors were stabilized followed by impregnated with DAHP as a flame retardant and carbonized at several high temperatures. The results showed that the carbon yield, thermal properties, and tensile strength of the material formed from lyocell fibers was higher compared to the material from viscose rayon fibers.

Rhim *et al.* (2010) showed that the electrical conductivity regions are directly linked to the microstructural changes during the cellulose-to-carbon conversion process, and the conductivity increases with rise in temperature up to 1200 °C (Rhim *et al.* 2010). Sim *et al.* (2014) studied the electrical properties of cellulose-based carbon fiber and found that the higher cellulose content and lower the impurities enhance the electrical

conductivity of the fiber; the electrical properties increase with increasing carbonization temperature up to 1100 °C (Sim et al. 2014).

In this study, bacterial cellulose was used as a precursor of carbon nanofiber, and for the first time, the effect of using flame retardant and the variation in the heating rates of stabilization were studied simultaneously. Finally, the stabilized samples were carbonized at two temperatures (800 and 1200 °C) with two rates of heating (2 and 10 °C min^{-1}) in an inert atmosphere. Then changes in morphology, structure, and properties of the precursor and products during various stages of carbon fiber preparation were measured with various characterization equipment such as Scanning Electron Microscopy (SEM), Fourier Transform Infrared Spectroscopy (FTIR), X-ray Diffraction (XRD), Thermogravimetric Analysis (TGA), Differential Scanning Calorimetry (DSC), and electrical characteristics. The results elucidate the effect of flame retardant, heating rates of stabilization and carbonization temperature on carbon yield and electrical conductivity of resulted carbon nanofiber.

EXPERIMENTAL

Preparation of Cellulosic Nanofiber Precursor

Acetobacter xylinum was used as a bacterial cellulose producer in liquid culture media. The culture media included a modified HS medium (D-Glucose, 20 g/L; yeast extract, 5 g/L; cornsteep liquor, 5 g/L; Na_2HPO_4, 2.7 g/L; and citric acid, 1.15 g/L); and medium of equal composition plus 1% ethanol. The yield of the cultured BC was 5.43 g/L (per liter of culture media). Bacterial cellulose layers formed on surface of the liquid during 14 to 20 days at 30 °C under static conditions. Bacterial cellulose pellicles were extracted by centrifugation at 5000 rpm for 15 min. They were treated with 0.1M NaOH at 90 °C for 1 h to remove any remaining microorganisms, medium components, and soluble polysaccharides. Then the bacterial cellulose was centrifuged at 5000 rpm for 15 min again. The purified bacterial cellulose was then thoroughly washed with distilled water until a neutral pH was achieved. The nanofibrils were dispersed in distilled water using an electrical mixer and stirred by an electromagnetic stirrer for 1 day. Ultrasonic waves were applied to each solution for 7 min at 50 Hz. At the end, the desingrator was used at 3000 rpm to achieve better dispersion of nanofibers in water. The nanofibril suspension was prepared using a handsheet maker as a nonwoven sheet. The prepared sheet was dried at 40 °C for 1 day. The average thickness of the nanosheets was 50 microns.

Impregnation of Precursors with Flame Retardant

Diammonium phosphate ($(NH_4)_2HPO_4$, A-3 Okhla Industrial Area, phase-I, New Dehli-110 020 (INDIA) ISO 9001: 2000 certified company) was used as a flame retardant (25% by weight of dry substances calculated from the total weight of the fluid) to impregnate precursors by spraying on nanosheets before drying them (Valso *et al.* 2000).

Stabilization and Carbonization Methods

The precursor nanosheets were dried in an oven at about 103 °C for 24 h and then kept in a desiccator for humidity control before the stabilization process. All of the impregnated and pristine cellulosic nanofiber sheets were stepwise heat treated for 20

min at four temperatures (105, 150, 200, and 250 °C) with two different heating rates (2 and 10 °C min^{-1}) in an air atmosphere (Peng *et al.* 2003). The stabilized samples were carbonized at two temperatures (800 and 1200 °C) with two heating rates (2 and 10 °C min^{-1}) in an inert atmosphere.

Sample codes based on impregnation, stabilization, and carbonization conditions are shown in Table 1. The sample codes of P and I are attributed to pristine and impregnated cellulosic nanofiber sheets with DAP, respectively.

Table 1. Encoding of Samples

Sample	Impregnation		Stabilization (250 °C)		Carbonization			
					800 °C		1200 °C	
	Without DAP	With DAP	Heating rate 2 °C min^{-1}	Heating rate 10 °C min^{-1}	Heating rate 2 °C min^{-1}	Heating rate °C min^{-1} 10	Heating rate °C min^{-1} 2	Heating rate °C min^{-1} 10
P	*	-	-	-	-	-	-	-
I	-	*	-	-	-	-	-	-
PS2	*	-	*	-	-	-	-	-
IS2	-	*	*	-	-	-	-	-
IS10	-	*	-	*	-	-	-	-
PS2C2-800	*	-	*	-	*	-	-	-
IS2C2-800	-	*	*	-	*	-	-	-
IS10C10-800	-	*	-	*	-	*	-	-
IS2C2-1200	-	*	*	-	-	-	*	-
IS10C10-1200	-	*	-	*	-	-	-	*

Characterization of Cellulosic Precursor, Stabilized and Carbonized Samples

Chemical changes and functional groups of impregnated and pristine cellulosic and stabilized nanofiber sheets were investigated by Fourier transform infrared spectroscopy (FTIR-AVATAR 370, Thermo Nicolet). The spectra were recorded in the range of 400-4000 cm^{-1} using a potassium bromide tablet (Fluka Company).

The change in mass of impregnated and pristine cellulosic and stabilized nanofiber sheets was measured by thermogravimetric analysis (TGA) (American TA Model Q600) with a heating rate of 5 °C min^{-1} from room temperature to 1000 °C in an argon atmosphere. Thermal behavior of impregnated and pristine cellulosic and stabilized nanofiber sheets was studied by Differential Scanning Calorimetry (DSC) (Model Q600 manufactured by TA America) in an argon and air atmospheres at a heating rate of 5 °C min^{-1} from room temperature to 1000 °C.

Morphological characteristics of samples were evaluated by a scanning electron microscope (SEM) (FEI Quanta 200) at 25 kV. Prior to SEM observations, the samples were coated with a thin layer of gold to avoid charge accumulations.

The crystal related structural parameters were acquired using a wide-angle X-ray diffraction with Cu Kα radiation (wavelength λ=1/54 A°) over the range of $5°<2\Theta<80°$

with a step width of 0.02°. The operating voltage and current were 40 KV and 30 mA, respectively. The crystal size (L_c) was calculated by the Scherrer Eq. (1),

$$L_c = K\lambda/\beta\cos\theta \quad (1)$$

where λ is the wavelength of the X-ray, $\beta$is the half width of the diffraction peaks (FWHM), and k is the shape factor (0.94). Bragg's Eq. (2) was utilized to calculate the interlayer spacing,

$$d = \lambda/(2\sin\theta) \quad (2)$$

where Θ is the scattering angle of the peak position.

Electrical conductivity of the samples was measured by standard four-point probe method (according to ASTM D 257-99) using a Keithley 196 System DMM_2.

RESULTS AND DISCUSSION

FTIR Study of Cellulosic and Stabilized Cellulosic Nanofiber Sheets

The FTIR spectra of impregnated (I) and pristine (P) cellulosic nanofiber sheets and stabilized impregnated and stabilized pristine cellulosic nanofiber sheets (IS2 and PS2 stabilized at 250 °C with the heating rate of 2 °C min^{-1}) are shown in Fig. 2. The main FTIR characteristic bands of cellulosic and stabilized nanofiber sheets, their related functional groups, and the modes of vibrations are shown in Table 2.

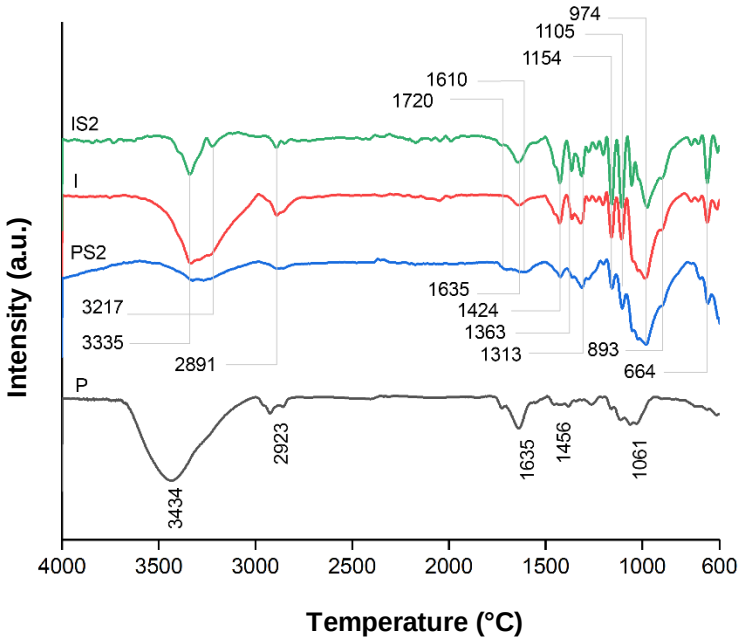

Fig. 2. FTIR spectra of initial (unstabilized) and stabilized cellulosic nanofiber sheets

As cellulose is a polysaccharide, it has many OH groups, and the very strong absorption band at 3434 cm^{-1} in the P sample is attributed to the OH stretching vibration of polysaccharide structure of precursor. Also, the band at 2923 cm^{-1} is attributed to C-H stretching vibration, whereas the band at 1635 cm^{-1} is assigned to OH stretching of

adsorbed water by samples. Absorption at 1456 cm^{-1} can be assigned to C-H symmetrical bending. Strong absorption at 1061 cm^{-1} is associated with asymmetric stretching vibration of C-O-C bonds in the pyranose ring structure of cellulose (Bali *et al.* 2013; Treesuppharat *et al.* 2017). For stabilized samples (PS2, IS2), the dehydration process causes a drop in intensity of OH stretching band at about 3400 cm^{-1}. Moreover, strong absorption around 974 cm^{-1} area can be attributed to the stretching vibration of many C-O and C-C bonds in the structure. The presence of peaks at 893 and 1105 cm^{-1} is ascribed to the stretching vibration at cellulose ring. The peaks in the range of lower than 900 cm^{-1} appear to be due to bending deformed states outside the bonds of C-OH and C-C (Fig. 2). In stabilized samples of PS2 and IS2 and during oxidation, bands at 1720 cm^{-1} and 1610 cm^{-1} are formed, which are attributed to C=O stretching and C=C stretching vibrations, respectively (Dumanli and Windle 2012; Frank *et al.* 2014). The bands at 1460, 3119, and 3217 cm^{-1} in I and IS2 samples are due to the presence of NH_4 groups in the diammonium phosphate as flame retardant.

Table 2. FTIR Spectral Results of Initial (unstabilized) and Stabilized Cellulosic Nanofiber Samples

Wavenumber (cm^{-1})	Functional groups and mode of vibration
3434	OH stretching
3119	NH_4 (DAP)
2923	CH stretching
1720	C=O stretching
1635	OH (adsorbed water)
1610	C=C
1460	NH_4 (DAP)
1456	CH bending and deformation
1061	C-O-C (pyranose ring)
893-1105	Vibration at β-glycosidic linkage
974	C-O , C-C stretching
900>	C-C, C-O (out of plane)

Study of Thermal Behavior

TGA

As shown in Fig. 3a, mass reduction in pristine (P) and impregnated (I) samples occurred in two separable stages. The degradation of sample I (297 °C) began at higher temperature compared to the P sample (140 °C), due to impregnation of I sample with $(NH_4)_2HPO_4$ as flame retardant but after that, the degradation of I sample occurred more severely. Hence, the mass reduction of I sample reached 52% at the temperature range of 297 to 400 °C. The reason for this behavior is that $(NH_4)_2HPO_4$ decomposes to a Lewis acid (phosphoric acid) during heating treatment (Mack and Donalson 1967). It seems that the primary decomposition of a flame retardant requires higher energy, which is provided at temperatures around 300 °C, and no significant weight loss is observed below 300 °C. However, this phenomenon occurs in a pristine (P) at about 200 °C. Therefore, the presence of a flame retardant resulted in a significant difference of about 100 °C. After decomposition, the resulting acid (H_3PO_4) acts as a catalyst and accelerates the

dehydration of cellulose, allowing the possibility of a covalent cross-link formation between the adjacent monomeric repeat groups of glucose (Back 1967).

In Fig. 3b, in PS2 (stabilized pristine cellulosic nanofiber sheet at the heating rate of 2 °C min^{-1}), the starting temperature of degradation (222 °C) was higher than for the P sample (140 °C). As PS2 underwent the stabilization process at 2 °C min^{-1} heating rate, the first dehydration took place during the thermal treatment and stabilization reactions to some extent (compared to P). Thus, because of the initial structural consolidation in the stabilization of PS2, the occurrence of new reactions began at higher temperature (220 °C). Comparing PS2 and P samples revealed that the mechanism of weight loss in the PS2 sample was different, which is attributable to the thermal breakdown of C-C and C-O groups and also the formation and emission of some volatile compounds such as H_2O, CO and CO_2 (Tang and Bacon 1964). In the P sample, a combination of these products was emitted with a lower slope, which can be explained, according to the pyrolysis mechanism in stage 3a of Fig. 1.

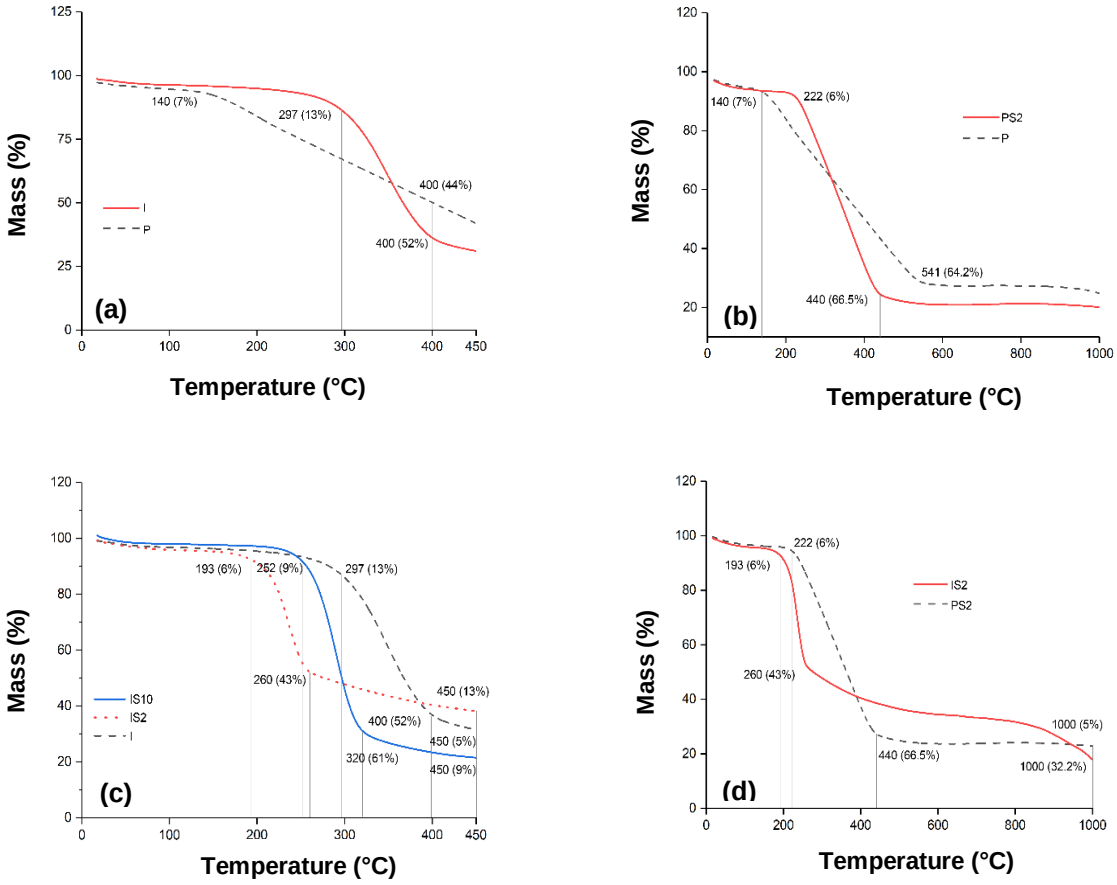

Fig. 3. TGA curves of a) impregnated (I) and pristine (P) cellulosic nanofiber sheets in argon, b) pristine (P) and stabilized pristine (PS2) cellulosic nanofiber sheets in argon, c) impregnated (I) and stabilized impregnation at a heating rate of 2 and 10 °C min^{-1} (IS2 and IS10) cellulose nanofiber sheets in argon, d) impregnated and pristine cellulose nanofiber sheets at heating rate of 2 °C min^{-1} (IS2 and PS2) in argon

The TGA curves of impregnated cellulosic nanofiber sheet (I) and stabilized impregnated cellulosic nanofiber sheets at heating rates of 2 and 10 °C/min (IS2 and

IS10) are shown in Fig. 3c. Making a comparison between IS2 and IS10 TGA curves with the TGA curve of I sample shows that the beginning of IS2 degradation took place at a lower temperature than those of IS10 and I samples. While considering the effect of the heating rate, the IS2 sample should have a better and more complete stabilization. The reason for the weight loss difference between the samples is that lower heating rate and the longer time of stabilization process in IS2 sample, as well as the surface penetration of the flame retardant (DAP) into the sample, resulted in the maximum loss of flame retardant (DAP). Therefore, the thermal behavior of IS2 after stabilization was approximately close to the behavior of PS2 (at the initial degradation temperature). The start of degradation in IS2 sample occurred from 193 °C, but the IS10 sample began to lose weight at 252 °C. At the same time, the weight loss of IS2 was 43%, which is lower than weight loss in IS10. Thus, it can be concluded that the simultaneous use of flame retardant and low heating rate (2 °C min^{-1}) led to obtaining higher stability in cellulose nanofiber sheets. It seems that the proposed path for occurrence of chemical reactions tended toward the 3b path (in Fig. 1) in the pyrolysis mechanism.

Figure 3d presents the TGA curves of impregnated and pristine cellulosic nanofiber sheets at the heating rate of 2 °C min^{-1} (IS2 and PS2). Degradation of IS2 began at lower temperature with a steeper slope and higher intensity than that of PS2. The reason for this difference is that $(NH_4)_2HPO_4$ decomposes to phosphoric acid during heat treatment and H_3PO_4 accelerates the dehydration of cellulose, allowing the possibility of a covalent cross-link formation between two monomers of glucose (Back 1967). Mass reduction in IS2 occurred in three stages. According to the TGA curve of IS2 sample, it can be concluded that reducing the heating rate as well as simultaneous use of flame retardant can lead the stabilization reactions corresponding to the 3b path in Fig. 1 and prevent the formation of levoglucosan compounds.

TGA quantitative results of initial (unstabilized) and stabilized cellulosic nanofiber sheets are shown in Table 3. According to the results presented in Table 3, it can be concluded that the heating rate of 10 °C min^{-1}, was not suitable for stabilizing cellulosic nanofiber sheets due to its high weight loss. Flame retardant materials with two mechanisms for removing OH groups or reacting with OH groups provide thermal stability of cellulosic sheets and reduce the rate of chemical decomposition reactions. As the heating rate rises, the effect of the flame retardant disappears, and this material plays a better role in lower heating rates.

Table 3. TGA Results of Initial (unstabilized) and Stabilized Samples

Sample	First mass Reduction Temperature Range (°C)	First mass loss (%)	Second Mass Reduction Temperature Range (°C)	Second Mass Loss (%)	Third Mass Reduction Temperature Range (°C)	Third Mass Loss (%)
P-ar	Room temp to 140	7	140 to 541	64.2	541 to 1000	3.9
I-ar	Room temp to 297	13	297 to 400	52	400 to 450	5
PS2-ar	Room temp to 222	6	222 to 440	66.5	440 to 1000	4.9
IS2-ar	Room temp to 193	6	193 to 260	43	260 to 1000	32.3
IS10-ar	Room temp to 252	6	252 to 320	61	320 to 1000	21

The dehydration stage takes place at a specified rate up to the temperature of less than 250 °C and stabilizes the cellulose structure, while the decomposition reactions occur at temperatures above 250 °C. If the dehydration of the cellulose structure is not fully completed at initial temperatures, de-polymerization in the early stages of stabilization process leads to shrinkage, the formation of volatile particles, and ultimately leads to lose large amounts of weight at higher temperatures (Brunner and Roberts 1980). Therefore, the carbon yield can be increased by using slow heating rates.

DSC

DSC curves of cellulosic nanofiber sheets are shown in Fig. 4, and their quantitative results are presented in Table 4. The DSC curves of pristine (P) and impregnated (I) cellulosic nanofiber sheets in air (Fig. 4a) show an maximum peak around 338 °C for P sample and an maximum peak at about 327 °C in I sample. The presence of flame retardant in I sample shifts the initiation temperature of the stabilization reactions to a lower temperature (200 °C). By contrast, in the pristine P, the reactions are initiated at 309 °C. In Fig. 4b, the DSC curves of pristine (P) and saturated (I) cellulosic nanofiber sheets in inert atmosphere (argon) show an maximum peak around 555 °C (P sample), which can be attributed to the partial pyrolysis due to fragmentation of carbonyl and carboxylic bonds from anhydrous glucoses units, giving carbon or monoxide carbon (Barud *et al.* 2007) and an maximum peak at about 302 °C (I sample). Also, different enthalpy of two samples (P and I) can be observed clearly, in which impregnation process causes a sharp decrease in the maximum peak temperatures (555 °C against 302 °C).

In Fig. 4c, the amount of enthalpy or energy released from the P sample is 2645 W g-1, and there was no significant difference with the enthalpy released in PS2 sample at 2599 W g^{-1}. This indicates that stabilized pristine samples at 250 °C actually did not make much progress in stabilizing reactions. In other words, if the stabilization reactions have appropriate progress, then there should be a significant difference in the enthalpy of these two samples. Therefore, it can be concluded that the presence of a flame retardant in the progress of stabilization reactions plays a very significant and determinant role.

Figure 4d shows the DSC curves of impregnated cellulose nanofiber sheet (I) and stabilized impregnated cellulosic nanofiber sheets at heating rates of 2 °C and 10 °C min-1 (IS2, IS10). The maximum peak temperature in IS2 and IS10 samples (stabilized impregnated nanofiber sheets), compared to I (initial nanofiber sheet without stabilization) under the DSC analysis was increased, and this indicates that the heat treatment in IS2 and IS10 contributed to structural stability and stabilization in fibers to some extent. At the same time, the maximum peak temperature in IS2 is shown at about 370 °C, while IS10 shows at 331 °C. This implies that IS2 needed higher temperatures (370 °C) for starting and progressing of stabilization reactions. In other words, as discussed in TGA and Fig. 1, the progress of stabilization reactions depends on the progress of molecular dehydration reaction of cellulose, which is higher at a lower heating rate and practically has not been done properly at the heating rate of 10 °C min^{-1}. Consequently, the material has begun to react and dehydrate in the DSC analysis at temperatures around 331 °C. The enthalpy of I is 6820 W g^{-1}, while IS2 and IS10 have approximately equal amount of enthalpy and about half of I. This indicates that stabilization reactions achieved appropriate progress in IS2 and IS10 samples. At the same time, the enthalpy of I, IS2, and IS10 samples was more than those of P and PS2.

Generally, the presence of flame retardant, at both heating rates of 2 and 10 °C min^{-1}, can help the stabilization reactions.

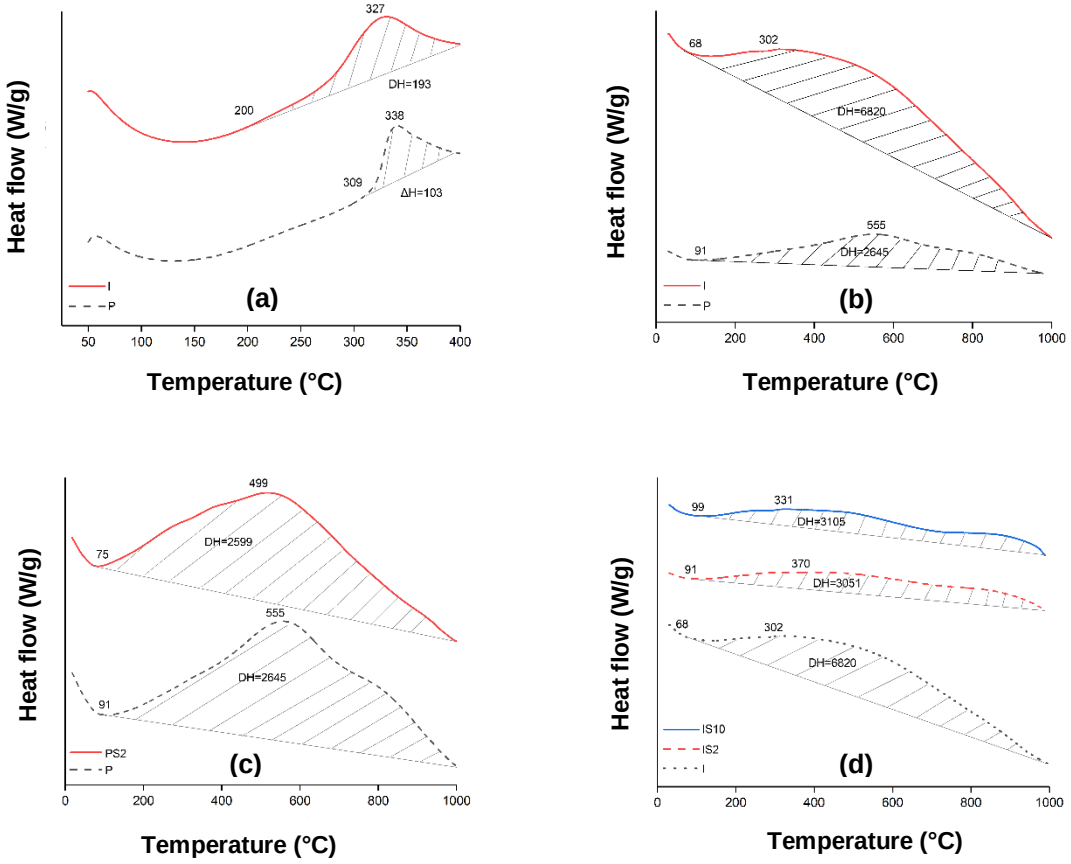

Fig. 4. DSC curves of a) impregnated (I) and pristine (P) cellulosic nanofiber sheets in air, b) impregnated (I) and pristine (P) cellulosic nanofiber Sheets in argon, c) pristine (P) and stabilized pristine (PS2) cellulosic nanofiber sheets in argon, d) impregnated (I) and stabilized impregnated at heating rates of 2 and 10 °C min^{-1} (IS2 and IS10) cellulose nanofiber sheets in argon

Table 4. DSC Results of Initial (unstabilized) and Stabilized Nanofiber Sheets

Sample	Onset temperature of peak (°C)	End temperature of peak (°C)	Temperature range of peak (°C)	Highest temperature peak	Δ*H* (W g^{-1})
P-air	309	400	91	338	103
I-air	200	400	200	327	193
P-ar	91	1000	909	555	2645
I-ar	68	1000	932	302	6820
PS2-ar	75	1000	925	499	2599
IS2-ar	91	1000	909	370	3051
IS10-ar	99	1000	901	331	3105

Morphological Characteristics

Nano-structure is observed in the SEM images (Fig. 5) of all samples including pristine cellulosic nanofiber sheet, stabilized, and carbonized nanofiber sheets.

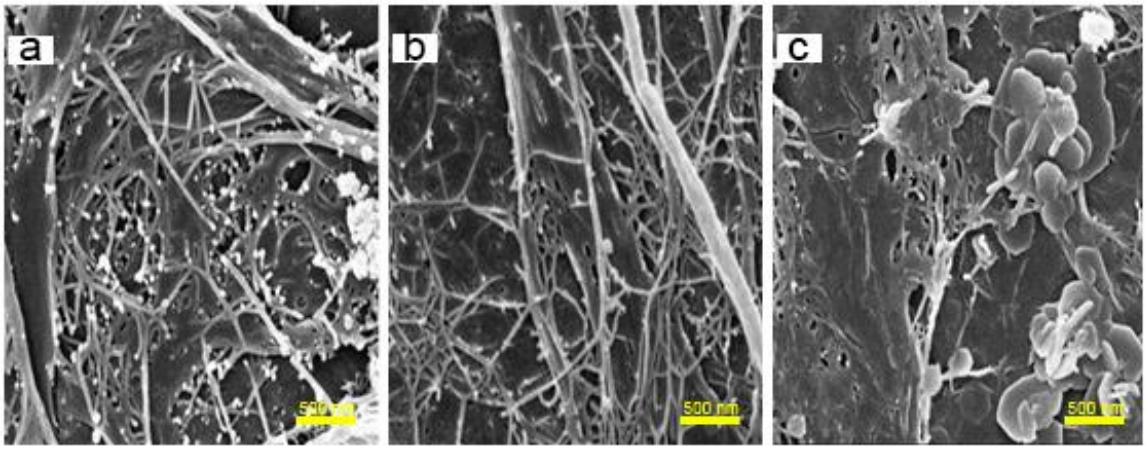

Fig. 5. SEM images of a) the P sample, b) the PS2 sample, and c) the PS2C2-800 sample (Magnification: 80000X)

According to the SEM images in Fig. 6, impregnated samples, including initial (unstabilized) nanofiber sheet and stabilized at both heating rates (2 and 10 °C min-1) and carbonized at 800 °C, exhibited a nano-fibrous structure and retained their nano-fibrous geometry under these heat treatments. However, raising the temperature of carbonization to 1200 °C at both heating rates changed the geometrical structure and the carbonized sheet became an integrated entity.

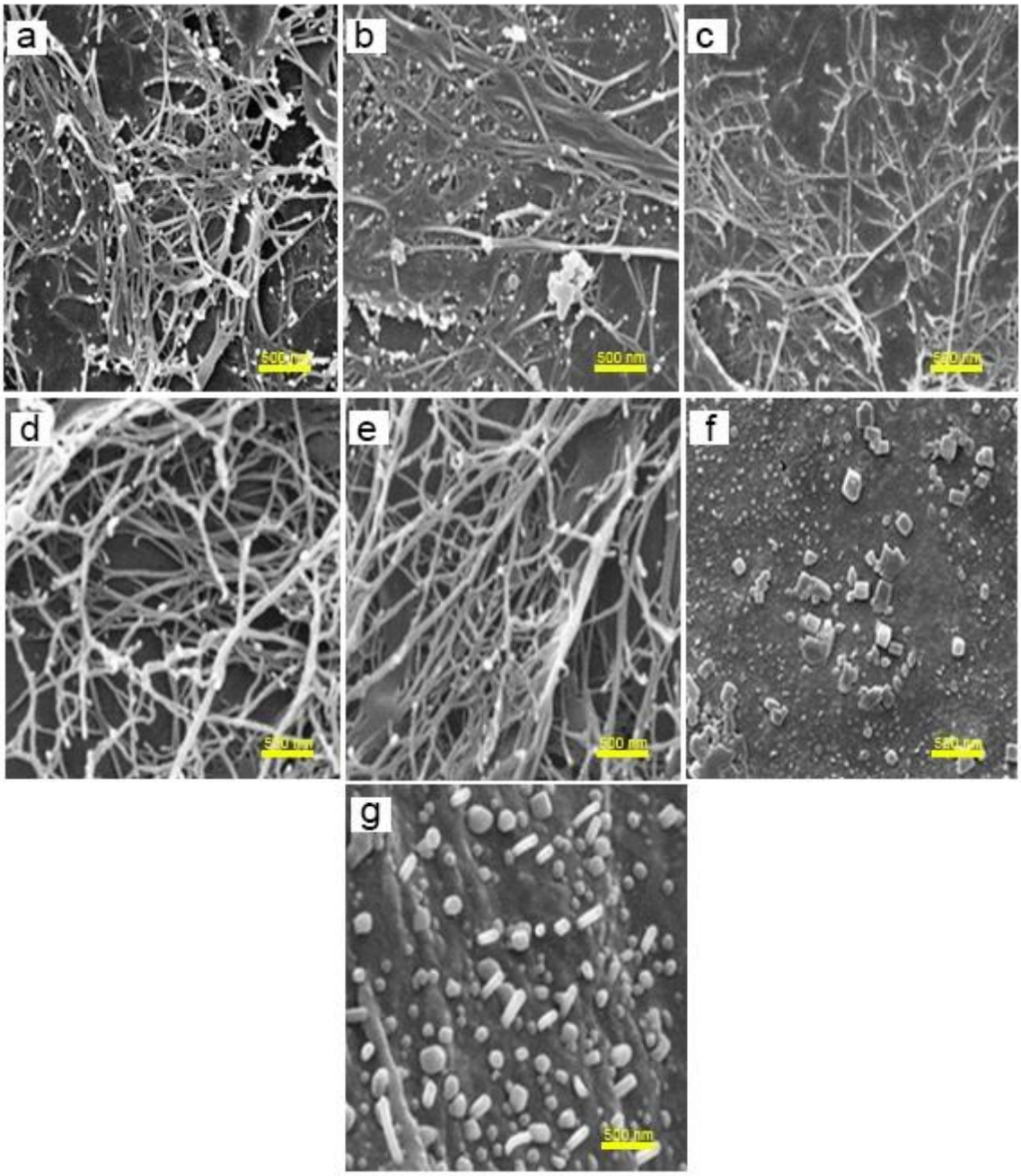

Fig. 6. SEM images of a) the I sample, b) the IS2 sample, c) the IS10 sample, d) the IS2C2-800 sample, e) the IS10C10-800 sample, f) the IS2C2-1200 sample, and g) the IS10C10-1200 sample (Magnification: 80000X)

Study of Crystalline Structure

The XRD patterns and resulting crystalline parameters of pristine, stabilized, and carbonized nanofiber sheets are shown in Fig. 7a and Table 5, respectively. There were three characteristic peaks in XRD pattern of pristine cellulose nanofiber sheet (P). The first peak was around 2Θ = 22°, and two other peaks were around 14° and 16°, which could be ascribed to reflections of (200), (110), and (110) planes, respectively (Bali *et al.* 2013; Santos *et al.* 2015; Treesuppharat *et al.* 2017). In the XRD patterns of PS2, IS2,

and IS10 (stabilized samples), these peaks appeared in similar 2Θ, with a slight shift in each diffraction (Fig. 7a). Also, the peak width (FWHM) in stabilized samples was lower than that of a pristine cellulosic nanofiber sample (P). The average size of crystals for P, PS2, IS2 and IS10 samples was 44.3, 96, 110, and 84.3 Ångstrom, respectively. Stabilization makes an increase in crystals size in both impregnated and pristine samples. However, the difference in the size of crystals in IS2 and IS10 nanofiber sheets is related to more progress of the stabilization reactions in IS2 sample (Table 5). Accordingly, the simultaneous effect of low heating rate and impregnation of flame retardant caused suitable pyrolysis mechanism (along the 3b path Fig. 1) as mentioned in the TGA results.

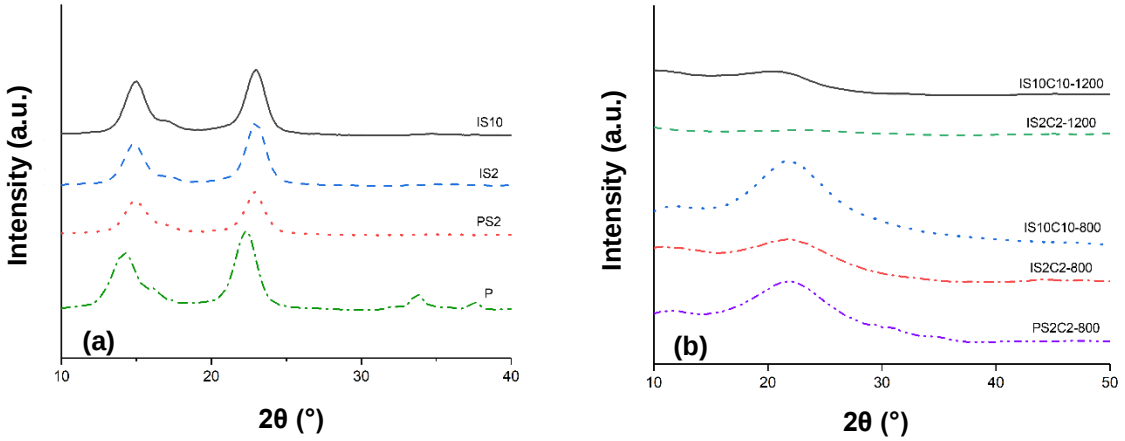

Fig. 7. X-ray diffraction patterns of a) pristine and stabilized, b) carbonized nanofiber sheets

Table 5. Structural Parameters of Pristine, Stabilized, and Carbonized Cellulosic Nanofiber Sheets

Sample	2Θ (°)	Intensity (a.u.)	FWHM (rad)	d (A°)	L_c (A°)
P	22.3	2961.6	0.033	3.99	44.3
PS2	22.9	1589.8	0.015	3.88	96
IS2	22.8	2281.32	0.014	3.88	110
IS10	22.9	2350.15	0.017	3.93	84.3
PS2C2-800	21.8	720.08	0.064	4.06	23
IS2C2-800	21.7	529.46	0.055	4.08	26.9
IS10C10-800	21.7	991.97	0.053	4.08	27.6
IS2C2-1200	22.6	96.61	0.112	3.92	13.2
IS10C10-1200	20.9	311.03	0.046	4.31	32.2

There was a characteristic peak at about 2Θ = 21-22° in the XRD curve of carbonized sheet, which is attributed to the reflection of (200) plane. However, a slight shift was observed in each diffraction. The average size of the crystals for PS2C2-800, IS2C2-800, IS10C10-800, IS2C2-1200, and IS10C10-1200 samples, was 23, 26.9, 27.6, 13.2, and 32.2 Ångstroms, respectively (Fig. 7b and Table 5). As the carbonization temperature increased, the average crystalline size of cellulosic nanofiber sheets

decreased, followed by arrangement of carbon atom from disorder to regular order (Ma *et al.* 2013).

Electrical Conductivity of Carbonized Cellulosic Nanofiber Sheets

The electrical conductivity of carbonized samples was measured, and the results are tabulated in Table 6. The electrical conductivity of PS2C2-800, IS2C2-800, IS10C10-800, IS2C2-1200, and IS10C10-1200 was determined to be 7.4, 4.5, 4.4, 80, and 2.5 Ms cm^{-1}, respectively. As the results show, the electrical conductivity of carbonized samples at 1200 °C was significantly higher than 800 °C. This result shows that the carbon structure was formed at a higher temperature. At temperatures of 1200 °C, a sample that carbonized at a heating rate of 2 °C min^{-1} exhibited a much higher electrical conductivity than the carbonized sample with a heating rate of 10 °C min^{-1}. This result may also be due to better formation of graphite plates in the nanofiber axis direction that carbonized at low heating rate. As shown in the SEM images, heat treatment at 1200 °C resulted in a change in the shape of the nano-fibrous entities, thus achieving a suitable surface morphology and an integrated structure that would lead to a better conduction of the electrons in the structure.

Table 6. Electrical Conductivity of Carbonized Cellulosic Nanofiber Sheet

Sample	Electric conductivity (mS/cm)
PS2C2-800	7.4
IS2C2-800	4.5
IS10C10-800	4.4
IS2C2-1200	80
IS10C10-1200	25

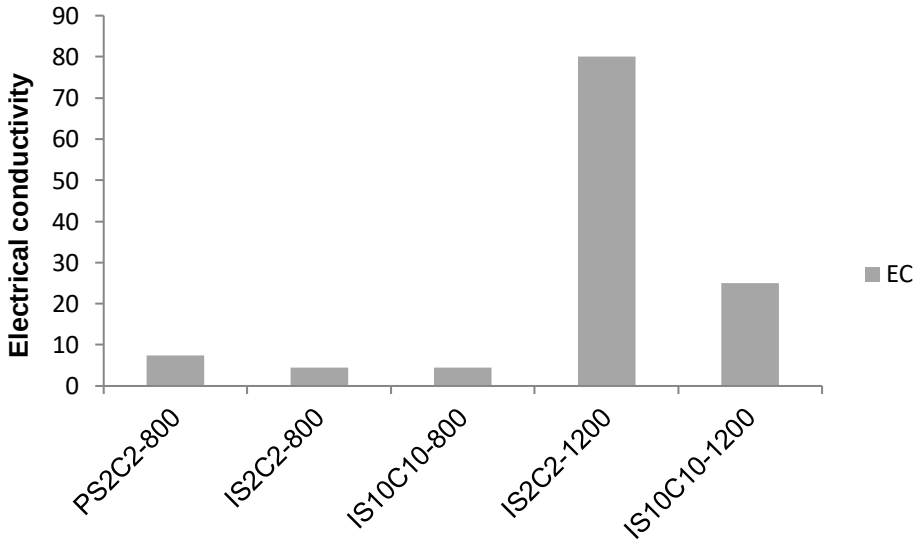

Fig. 8. Electrical conductivity of carbonized samples

CONCLUSIONS

1. This research confirmed that the bacterial cellulose, as a sustainable and renewable resource, can be employed as precursor for producing carbon fiber.
2. Simultaneous application of flame retardant and low heating rate (2 °C min^{-1}) synergically increased thermal stability and the carbon yield of cellulosic nanofiber sheets.
3. At low heating rate, increasing the carbonization temperature from 800 to 1200 °C led to the completion and growth of the carbon-graphite structure and increases electrical conductivity.
4. Finally, carbon nanofiber sheets resulted from impregnated samples at the higher temperature and the lower heating rate had more suitable thermal stability and electrical conductivity.

ACKNOWLEDGMENTS

Thanks for the support technical assistance of Dr. Habibollah Younesi in conducting this research.

REFERENCES CITED

Abba, M., Ibrahim, Z., Chong, C. S., Zawawi, N. A., Kadir, M. R. A., Yusof, A. H. M., and Razak, S. I. A. (2019). "Transdermal delivery of crocin using bacterial nanocellulose membrane," *Fiber. Polym.* 20(10), 2025-2031. DOI: 10.1007/s12221-019-9076-8

Arbab, S., Mirbaha, H., Zeinolebadi, A., and Nourpanah, P. (2014). "Indicators for evaluation of progress in thermal stabilization reactions of polyacrylonitrile fibers," *J. Appl. Polym. Sci.* 131(1), 1-8. DOI: 10.1002/app.40343

Arbab, S., Teimoury, A., Mirbaha, H., Adolphe, D. C., Noroozi, B., and Nourpanah, P. (2017). "Optimum stabilization processing parameters for polyacrylonitrile-based carbon nanofibers and their difference with carbon (micro) fibers," *Polym. Degrad. Stab.* 142, 198-208. DOI: 10.1016/j.polymdegradstab.2017.06.026

Arbab, S., and Zeinolebadi, A. (2013). "A procedure for precise determination of thermal stabilization reactions in carbon fiber precursors," *Polym. Degrad. Stab.* 98(12), 2537-2545. DOI: 10.1016/j.polymdegradstab.2013.09.014

Back, E. L. (1967). "Thermal auto-crosslinking in cellulose material," *Pulp Paper Mag. Can.* 68(4), 165-171.

Bali, G., Foston, M. B., O'Neill, H. M., Evans, B. R., He, J., and Ragauskas, A. J. (2013). "The effect of deuteration on the structure of bacterial cellulose," *Carbohydr. Res.* 374, 82-88. DOI: 10.1016/j.carres.2013.04.009

Barud, H., Ribeiro, C., Crespi, M., Martines, M., Dexpert-Ghys, J., Marques, R., Messaddeq, Y., and Ribeiro, S. (2007). "Thermal characterization of bacterial cellulose–phosphate composite membranes," *J. Therm. Anal. Calorim.* 87(3), 815-818.

Brunner, P. H., and Roberts, P. V. (1980). "The significance of heating rate on char yield and char properties in the pyrolysis of cellulose," *Carbon*, 18(3), 217-224. DOI: 10.1016/0008-6223(80)90064-0

Castro, C., Zuluaga, R., Putaux, J.-L., Caro, G., Mondragon, I., and Gañán, P. (2011). "Structural characterization of bacterial cellulose produced by *Gluconacetobacter swingsii* sp. from Colombian agroindustrial wastes," *Carbohydr. Polym.* 84(1), 96-102. DOI: 10.1016/j.carbpol.2010.10.072

Chanzy, H., Paillet, M., and Hagege, R. (1990). "Spinning of cellulose from N-methyl morpholine N-oxide in the presence of additives," *Polymer*, 31(3), 400-405. DOI: 10.1007/s13233-010-0404-5

Chen, P., Cho, S. Y., and Jin, H.-J. (2010). "Modification and applications of bacterial celluloses in polymer science," *Macromol. Res.* 18(4), 309-320. DOI: 10.1007/s13233-010-0404-5

Dahman, Y., Jayasuriya, K. E., and Kalis, M. (2010). "Potential of biocellulose nanofibers production from agricultural renewable resources: preliminary study," *Appl. Biochem. Biotechnol.* 162(6), 1647-1659. DOI: 10.1007/s12010-010-8946-8

Donnet, J., and Bansal, R. (1984). "Surface properties of carbon fibers," in: *Carbon Fibers*, M. Dekker Inc., New York, NY.

Dumanlı, A. G., and Windle, A. H. (2012). "Carbon fibres from cellulosic precursors: A review." *J. Mater. Sci.* 47(10), 4236-4250. DOI: 10.1007/s10853-011-6081-8

El-Saied, H., Basta, A. H., and Gobran, R. H. (2004). "Research progress in friendly environmental technology for the production of cellulose products (bacterial cellulose and its application)," *Polym.-Plast. Technol. Eng.* 43(3), 797-820. DOI: 10.1081/PPT-120038065

Frank, E., Steudle, L. M., Ingildeev, D., Spoerl, J. M., and Buchmeiser, M. R. (2014). "Carbon fibers: Precursor systems, processing, structure, and properties," *Angew. Chem. Int. Ed.* 53(21), 5262-5298. DOI: 10.1002/anie.201306129

Karacan, I., and Soy, T. (2013). "Structure and properties of oxidatively stabilized viscose rayon fibers impregnated with boric acid and phosphoric acid prior to carbonization and activation steps," *J. Mater. Sci.* 48(5), 2009-2021. DOI: 10.1007/s10853-012-6970-5

Keshk, S. M. (2014). "Bacterial cellulose production and its industrial applications," *J. Bioprocess. Biotech.* 4(2), 1-16. DOI: 10.4172/2155-9821.1000150

Kilzer, F. J., and Broido, A. (1965). "Speculations on the nature of cellulose pyrolysis," *Pyrodynamics* 2, 151-163.

Koslow, E. E. (2007). "Carbon or activated carbon nanofibers," US Patent No. 7,296,691.

Lewin, M. (2006). *Handbook of Fiber Chemistry*, CRC Press, New York, NY.

Li, H., Yang, Y., Wen, Y., and Liu, L. (2007). "A mechanism study on preparation of rayon based carbon fibers with $(NH_4)\ 2SO_4$/NH4Cl/organosilicon composite catalyst system," *Compos. Sci. Technol.* 67(13), 2675-2682. DOI: 10.1016/j.compscitech.2007.03.008

Ma, X., Yuan, C., and Liu, X. (2014). "Mechanical, microstructure and surface characterizations of carbon fibers prepared from cellulose after liquefying and curing," *Materials* 7(1), 75-84. DOI: 10.3390/ma7010075

Mack, C. H., and Donaldson, D. J. (1967). "Effects of bases on the pyrolysis of cotton cellulose," *Text. Res. J.* 37(12), 1063-1071. DOI: 10.1177/004051756703701209

Madorsky, S. L. (1967). Termicheskoje Razloshenie Organischeskikh Polimerov. MIR Moscow, Moscow.

Mirbaha, H., Arbab, S., Zeinolebadi, A., and Nourpanah, P. (2013). "An investigation on actuation behavior of polyacrylonitrile gel fibers as a function of microstructure and stabilization temperature," *Smart Mater. Struct.* 22(4), 045019. DOI: 10.1088/0964-1726/22/4/045019

Nosratian Sabet, E., Nourpanah, P., and Arbab, S. (2016). "Quantitative analysis of entropic stress effect on the structural rearrangement during pre-stabilization of PAN precursor fibers," *Polymer* 90, 138-146. DOI: 10.1016/j.polymer.2016.03.001

Pappa, A., Mikedi, K., Tzamtzis, N., and Statheropoulos, M. (2003). "Chemometric methods for studying the effects of chemicals on cellulose pyrolysis by thermogravimetry–mass spectrometry," *J. Anal. Appl. Pyrol.* 67(2), 221-235. DOI: 10.1016/S0165-2370(02)00063-3

Peng, S., Shao, H., and Hu, X. (2003). "Lyocell fibers as the precursor of carbon fibers," *J. Appl. Polymer. Sci.* 90(7), 1941-1947. DOI: 10.1002/app.12879

Rafiei, S., Noroozi, B., Arbab, S., and Haghi, A. (2014). "Characteristic assessment of stabilized polyacrylonitrile nanowebs for the production of activated carbon nano-sorbents," *Chin. J. Polym. Sci.* 32(4), 449-457. DOI: 10.1007/s10118-014-1410-4

Rhim, Y.-R., Zhang, D., Fairbrother, D. H., Wepasnick, K. A., Livi, K. J., Bodnar, R. J., and Nagle, D. C. (2010). "Changes in electrical and microstructural properties of microcrystalline cellulose as function of carbonization temperature," *Carbon* 48(4), 1012-1024. DOI: 10.1016/j.carbon.2009.11.020

Saibuatong, O.-a., and Phisalaphong, M. (2010). "Novo aloe vera–bacterial cellulose composite film from biosynthesis," *Carbohydr. Polym.* 79(2), 455-460. DOI: 10.1016/j.carbpol.2009.08.039

Salihu, R., Foong, C. Y., Razak, S. I. A., Kadir, M. R. A., Yusof, A. H. M., and Nayan, N. H. M. (2019). "Overview of inexpensive production routes of bacterial cellulose and its applications in biomedical engineering," *Cell. Chem. Technol*. 53(1-2), 1-13.

Santos, S. M., Carbajo, J. M., Quintana, E., Ibarra, D., Gomez, N., Ladero, M., Eugenio, M. E., and Villar, J. C. (2015). "Characterization of purified bacterial cellulose focused on its use on paper restoration," *Carbohydr. Polym.* 116, 173-181. DOI: 10.1016/j.carbpol.2014.03.064

Schuyten, H., Weaver, J., and Reid, J. D. (1955). "Effect of flameproofing agents on cotton cellulose," *Ind. Eng. Chem.* 47(7), 1433-1439. DOI: 10.1021/ie50547a049

Shah, N., Ul-Islam, M., Khattak, W. A., and Park, J. K. (2013). "Overview of bacterial cellulose composites: A multipurpose advanced material," *Carbohydr. Polym.* 98(2), 1585-1598. DOI: 10.1016/j.carbpol.2013.08.018

Shindo, A., Nakanishi, Y., and Soma, I. (1969). "Carbon fibers from cellulose fibers," *J. Appl. Polym. Sci. Appl. Polym. Symp.* 9, 271-284.

Sim, I. N., Han, S. O., Kim, H., Han, I. S., Kim, S., Seo, D. W., Seong, Y.-H., and Foord, J. (2014). "Electrical properties of cellulose-based carbon fibers investigated using atomic force microscopy," *Macromol. Res.* 22(9), 996-1003. DOI: 10.1007/s13233-014-2130-x

Spörl, J. M., Beyer, R., Abels, F., Cwik, T., Müller, A., Hermanutz, F., and Buchmeiser, M. R. (2017). "Cellulose-derived carbon fibers with improved carbon yield and mechanical properties," *Macromol. Mater. Eng.* 302(10), 1700195. DOI: 10.1002/mame.201700195

Statheropoulos, M., and Kyriakou, S. (2000). "Quantitative thermogravimetric-mass spectrometric analysis for monitoring the effects of fire retardants on cellulose

pyrolysis," *Anal. Chim. Acta.* 409(1-2), 203-214. DOI: 10.1016/S0003-2670(99)00859-4

Tang, M. M., and Bacon, R. (1964). "Carbonization of cellulose fibers—I. Low temperature pyrolysis," *Carbon*, 2(3), 211-220. DOI: 10.1016/0008-6223(64)90035-1

Treesuppharat, W., Rojanapanthu, P., Siangsanoh, C., Manuspiya, H., and Ummartyotin, S. (2017). "Synthesis and characterization of bacterial cellulose and gelatin-based hydrogel composites for drug-delivery systems," *Biotechnol. Rep.* 15, 84-91. DOI: 10.1016/j.btre.2017.07.002

Valso, A., and Kleven, E. (2000). "Fire retarding composition and a method for impregnation of a combustible material," United States Patent 6,042,639.

Weil, E. D., and Levchik, S. V. (2008). "Flame retardants in commercial use or development for textiles," *J. Fire Sci.* 26(3), 243-281. DOI: 10.1177/0734904108089485

Wu, Q., and Pan, D. (2002). "A new cellulose based carbon fiber from a lyocell precursor," *Text. Res. J.* 72(5), 405-410. DOI: 10.1177/004051750207200506

Zhang, H., Guo, L., Shao, H., and Hu, X. (2006). "Nano-carbon black filled Lyocell fiber as a precursor for carbon fiber," *J. Appl. Polym. Sci.* 99(1), 65-74. DOI: 10.1002/app.22184

Zhu, H., Jia, S., Yang, H., Tang, W., Jia, Y., and Tan, Z. (2010). "Characterization of bacteriostatic sausage casing: A composite of bacterial cellulose embedded with ε-polylysine," *Food Sci. Biotechnol.* 19(6), 1479-1484. DOI: 10.1007/s10068-010-0211-y

Article submitted: October 23, 2019; Peer review completed: January 31, 2020; Revised version received: February 21, 2020; Accepted: February 22, 2020; Published: March 25, 2020.
DOI: 10.15376/biores.15.2.3408-3426